Materials Letters 147 (2015) 12–15

Contents lists available at ScienceDirect

Materials Letters

journal homepage: www.elsevier.com/locate/matlet

Large scale hydrothermal synthesis of monodisperse hexagonal WO_3 nanowire and the growth mechanism

Bin Miao [a], Wen Zeng [a,*], Shahid Hussain [a], Qiuping Mei [b], Sibo Xu [a], He Zhang [a], Yanqiong Li [a], Tianming Li [a]

[a] *College of Materials Science and Engineering, Chongqing University, Chongqing 400030, China*
[b] *Mechanical Engineering College, Nanchang Institute of Science & Technology, Nanchang 330108, China*

ARTICLE INFO

Article history:
Received 23 December 2014
Accepted 5 February 2015
Available online 14 February 2015

Keywords:
h-WO_3
Nanowires
Nanoparticles
Crystal structure
Primary nanoparticle
Growth mechanism

ABSTRACT

Monodisperse hexagonal tungsten oxide (h-WO_3) nanowires were novelly prepared on a large scale by the hydrothermal method with the assistance of K_2SO_4 and Na_2SO_4. The morphologies and structures of the nanowires were characterized by X-ray diffraction (XRD), focused ion beam scanning electron microscopy (FIB-SEM) and high-resolution transmission electron microscopy (TEM). These nanowires with a diameter of 80 nm and high crystallinity are especially bundles-like structure, which are growth from primary particles with same growth direction of [001] and the exposure to ⟨200⟩ facets. These primary nanoparticles are believed to have a crystal structure of hexagonal prism morphology. Based on the TEM characterizations and crystal structure analyses, the morphology evolvement and is given and the growth mechanism is discussed. This research is potentially applied to controlled synthesis 1D semiconductor oxides through hydrothermal route.

1. Introduction

Tungsten oxide (WO_3), one of the important semiconductor materials, is of great interest due to its promising physical and chemical properties [1,2]. As a wide band gap n-type semiconductor and due to the multiple oxidation states, WO_3 has been used to manufacture various devices such as electrochromic devices, gas sensors and photocatalysts cells [3–5]. Particularly, the hexagonal tungsten trioxide (h-WO_3) has attracted much attention during the past few years because of its hexagonal and trigonal tunnels [6,7]. And it has been widely used as an intercalation host for obtaining hexagonal tungsten bronzes M_xWO_3 ($M=Li^+$, Na^+, K^+, etc.) and promising materials for electrocatalyst and positive electrodes of lithium batteries [4,8].

Compared with bulk WO_3, 1D h-WO_3 nanostructures can show better sensitivity, fast electrochromic speed, high-contrast coloration, and high capacity retention. But these properties will be significantly influenced by the shape, size, and crystallinity of 1D h-WO_3 nanostructures [9,10]. Therefore, many efforts have been focused on the improvement of synthetic routes of 1D WO_3 nanostructures such as nanowires [11,12], nanorods, [13,14] nanotubes [15,16] and exploration of the 1D direction crystal growth mechanism [17,18]. However, except several report on the syntheses researches, there is still no deep understanding of the growth mechanism of 1D h-WO_3 nanostructures that can be widely accepted.

In this research, controlled synthesis of monodisperse h-WO_3 nanowire was carried out in hydrothermal conditions with sulfate salts as capping agent. Based on electron microscope observation, X-ray diffraction analyses, crystal structure characterization and analysis, a possible growth mechanism was given for h-WO_3 nanowires.

2. Experimental section

All chemical reagents were of analytic purity and used directly without further purification. To prepare h-WO_3 nanowire, 7 mmol of $Na_2WO_4 \cdot 2H_2O$, 1.75 mmol Na_2SO_4 and 1.75 mmol K_2SO_4 was dissolved in 40 ml deionized water under constant stirring, pH value was adjusted to 1.5–2.0 by the addition of HCl aqueous solution (2 M). The mixture was then transferred into a 50 ml Teflon-lined stainless steel autoclave, sealed, heated in oven at 180 °C for 24 h. After naturally cooled down to room temperature, the yellow precipitates were collected by centrifugation and washed with deionized water and ethanol for several times, and dried in vacuum at 60 °C for more than 4 h.

The crystal structure was determined by X-Ray Diffraction (XRD), a Rigaku D/Max- 1200X diffractometry equipped with Cu Kα radiation and a 2θ scanning rate of $0.02\,^\circ\,s^{-1}$ ranging from 10° to 60°. The morphologies and microstructures were analyzed by

---

[*] Corresponding author. Tel.: +86 23 65102465; fax: +86 23 65102465.
E-mail address: wenzeng@cqu.edu.cn (W. Zeng).

http://dx.doi.org/10.1016/j.matlet.2015.02.020
0167-577X/

focused ion beam scanning electron microscopy (FIB/SEM, Zeiss Auriga) and transmission electron microscope (TEM, ZEISS, LIBRA200).

3. Results and discussions

The SEM image is shown in Fig. 1(a), which clearly shows that there exists a mount of nanowires with diameters around 80 nm and length up to 2.5 μm, and the aspect ratio can be ~30. These nanowires are monodisperse that have uniform size and single morphology. Interestingly, their outer peripheral face is unsmooth with a lot of linear pits along the nanowire. Fig. 1(b) is The XRD pattern of the WO_3 nanowires. The patterns clearly demonstrated that the sample was pure hexagonal WO_3 crystal, with lattice constants of $a=b=7.298$ Å $c=3.899$ Å, from the JCPDS card (No. 75-2187). No other peaks can be observed from this pattern, indicating high purity of the h-WO_3 nanowires. In addition, the narrow and strong peaks illustrate the high crystallinity of the obtained h-WO_3 nanowires.

The detailed observation and characterization on the morphology and structure was carried out using TEM, HRTEM and SAED, as shown in Fig. 2. The TEM image in Fig. 2(a) indicates that the diameter of h-WO_3 nanowire is not completely consistent at the middle part and the part near the end. Interestingly, deduced from the select area electronic diffraction pattern (inset), the crystal structure is not polycrystal, but single crystal or polycrystal gathered by isotropous nanostructures. From the HRTEM observation (Fig. 2(b and c)), many surface defects can be seen along the axial direction of nanowire and not all the end faces of the primary nanowires are in the same plan. This can also certificate that the nanowire is budles-like structure, made of many isotropous 1D primary nanoparticles. On the other hand, the regular spacing of the lattice fringes is found to be about 0.391 nm and 0.316 nm (Fig. 2(c)), corresponding to the $\langle 001\rangle$ planes and $\langle 200\rangle$ planes, seperately. All this results confirm that the budles-like h-WO_3 nanowires are composed of primary wire-like single WO_3 growing along the $\langle 001\rangle$ directions and with the exposure of planes $\langle 200\rangle$. In addition, for the destination of exploring the time-depended reaction process of these nanowires, h-WO_3 nanowires were prepared by hydrothermal reaction at 180 °C for 8 h without any other synthesis conditions changed. As shown in Fig. 2(d), many dispersed nanowires with a diameter of ~10 nm were prepared.

For deep understand the growth mechanism, the h-WO_3 crystal structure (Fig. 3(a)) is built based on h-WO_3 JCPDS card (No. 75-2187), which has a space group of P6/mmm. According to the calculation by the Bravais–Friedel Donnay–Harker (BFDH) method [19], crystal morphology based on the crystal cell can be generated as a regular hexagonal prism with the exposure (001) planes and (100), (010), (1–10) planes during nucleation, as shown in Fig. 3(b) [17]. It can be deduced that, the h-WO_3 nanowires budles obtained in this research are grown from primary particles with hexagonal prism morphology.

Then the crystal structure of this primary nanoparticle with hexagonal prism morphology is given as Fig. 3(c–e). According to the research of Balaji et al. [6], the WO_6 octahedra (Fig. 3(c)) can form three- and six-membered rings by sharing the equatorial oxygen in the ab plane (001) and then stack by sharing the axial oxygen in the c axis [001]. Viewed from its [001] crystal direction (Fig. 3(d)) and [010] direction (Fig. 4(e)), a lot of hexagonal and trigonal tunnels are distributed. The insertion of cations such as

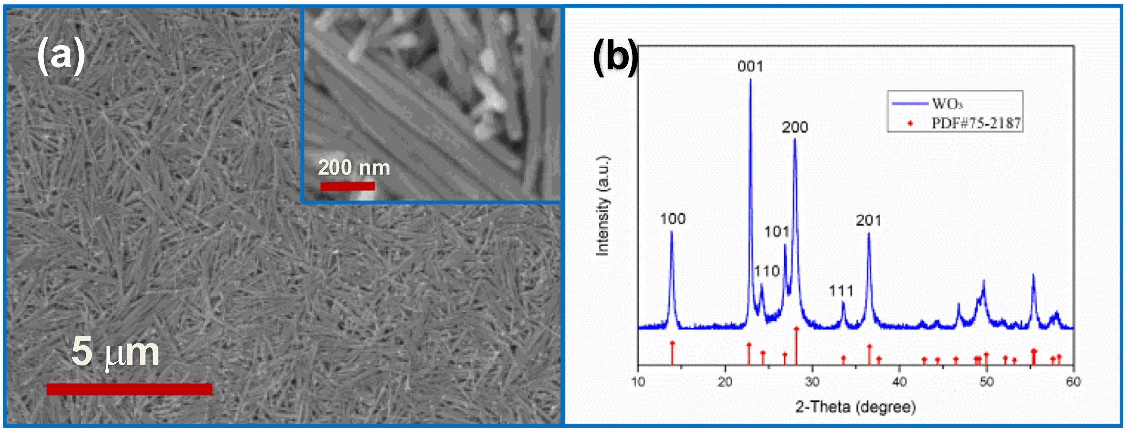

Fig. 1. SEM images and (b) XRD patterns of the h-WO_3 nanowires obtained at 180 °C for 24 h.

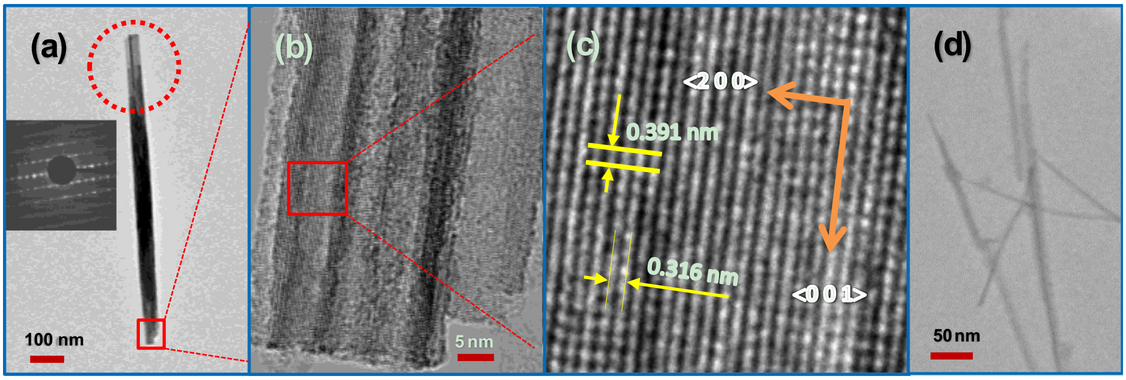

Fig. 2. (a)TEM, (inset) SAED, (b) HRTEM and (c) enlarged HRTME images of the h-WO_3 nanowires obtained at 180 °C for 24 h, (d) TEM images of h-WO_3 nanowires obtained at 180 °C for 8 h.